

Mass-action driven conformational switching of proteins: investigation of beta-lactoglobulin dimerisation by infrared spectroscopy

This content has been downloaded from IOPscience. Please scroll down to see the full text.

2015 J. Phys. D: Appl. Phys. 48 384001

(<http://iopscience.iop.org/0022-3727/48/38/384001>)

View [the table of contents for this issue](#), or go to the [journal homepage](#) for more

Download details:

IP Address: 131.211.105.126

This content was downloaded on 01/12/2015 at 09:45

Please note that [terms and conditions apply](#).

Mass-action driven conformational switching of proteins: investigation of beta-lactoglobulin dimerisation by infrared spectroscopy

Joris Stegen^{1,2}, John Ioannou³, Hans Tromp^{2,4}, Athene Donald³ and Paul van der Schoot^{1,2}

¹ Department of Applied Physics, Eindhoven University of Technology, Eindhoven, 5600 MB, The Netherlands

² Institute for Theoretical Physics, Utrecht University, Leuvenlaan 4, 3584 CE, Utrecht, The Netherlands

³ Sector of Biological & Soft Systems, Department of Physics, University of Cambridge, UK

⁴ NIZO Food Research, Ede, The Netherlands

E-mail: Hans.Tromp@NIZO.com

Received 7 April 2015, revised 28 May 2015

Accepted for publication 2 June 2015

Published 25 August 2015



Abstract

We study the dimerisation of beta-lactoglobulin (type A) at concentrations between 10 mg ml^{-1} and 200 mg ml^{-1} at fixed pH 3 and an ionic strength of 1.2 M and show that the degree of dimerisation can be determined from the coherent change in the ATR FTIR spectrum due to changes in folding induced by the dimerisation. This allows us to determine the IR spectrum of monomeric BLG and the dimerisation constant for which we find a value of $K = 1.84 (\pm 0.5) \cdot 10^2 \text{ M}^{-1}$. Furthermore, we show that including self-crowding effects at high concentrations accounts for the concentration dependence of the apparent dimerisation constant.

Keywords: protein, crowding, dimerisation

(Some figures may appear in colour only in the online journal)

1. Introduction

In the dairy industry there is a practical interest in understanding the fundamental physical interactions between hydration water molecules and whey proteins, which are widely used as ingredients in foods because of their functional properties, i.e. their emulsification, gelation, thickening, foaming and water-binding capacity [1, 2]. A fundamental problem that the food industry faces in formulating high-protein products, is that the stability and sensory qualities of these products irreversibly deteriorate if the protein content exceeds a certain percentage, the precise value of which depends on the application and the type of protein. Presumably, the process underlying this problem is a mass-action driven stabilisation of a dominant protein conformation that self-associates to form poorly soluble aggregates that lead to the deterioration

of the sensory qualities of food products with increasing protein content.

In this study we investigate this process experimentally on bovine beta-lactoglobulin (BLG) Type A. BLG is the major whey protein of cow and goat milk and a common ingredient of high-protein foods. BLG is a widely studied protein albeit that most research has either focused on structural transitions of BLG induced by changes in pH, heat treatment or the effects of ionic shielding with addition of various salts [3–6]. Moreover, many (if not all) previous studies that address aggregation ignore aggregation-induced structural changes. In this work, we investigate the aggregation through the spectroscopic characterisation of the induced structural changes in BLG at a fixed pH of 3, away from the isoelectric point of BLG of at pH 5.3 [3], at a fixed ionic strength of 1.2 M. We stress that we do not invoke any heat treatment so we focus on

aggregation that should be reversible in principle, arising as an effect of concentration.

As we perform experiments at a fixed pH of 3, we expect a concentration-dependent equilibrium between BLG in the monomeric and in the dimeric state. Higher levels of aggregation are extremely unlikely, as the dimer-octamer equilibrium for BLG (type A) is at pH 4.7 and the monomer-dimer equilibrium at pH 2.5 [4]. Only around pH 4.7, larger oligomeric structures have been reported to form, a process that is enhanced by a decrease in temperature and a decrease in ionic strength [3]. Consequently, our model system allows us to investigate the mass-action-driven dimerisation and the corresponding changes in secondary structure. Understanding such concentration-driven aggregation helps reveal the important generic processes which may play a part in protein responses, although the dimerisation of BLG is not a significant contributor to the deterioration of the sensory quality of high-protein food products.

We first discuss sample preparation and details of the ATR FTIR spectroscopy measurements in section 2. In section 3 we show that the monomeric IR spectrum of BLG can be determined and from that the concentration-dependent degree of dimerisation can be extracted by fitting a linear combination of the IR spectra of monomeric and dimeric BLG to the IR spectra measured at different concentrations. This contrasts with the conventional analysis of ATR FTIR measurements, where certain parts of the spectrum are associated with the presence of different types of secondary structure. In our approach, we use the coherent change in all types of secondary structure between two different dominant conformations, i.e. the conformation in the monomeric and dimeric state of BLG, to quantitatively determine the concentration-dependent equilibrium between these two conformations.

In section 3 we set up a dimerisation model that accounts for self-crowding effects and that explicitly takes into account the increase in free volume of the solution upon dimerization of the proteins. In section 4 we fit the model to the concentration-dependent degree of dimerisation and determine the dimerization constant as well as an effective hard-sphere radius that includes the effects of electrostatic interactions between the proteins. Excluded-volume interactions must be taken into account at the highest concentrations at which we performed experiments, because these produce degrees of dimerisation that are larger than those predicted by a simple mass-action model that does not account for effects of non-ideality. This confirms that crowding shifts the equilibrium of reactions towards the state with the smallest excluded volume, which for a monomer-dimer equilibrium is that towards the dimer state [7–9]. In section 5 we compare the obtained dimerisation constant with values previously reported in literature, and show that the obtained effective hard sphere radius is consistent with a theoretical prediction based on Debye-Hückel theory.

2. Materials and methods

Freeze-dried BLG type A (molar mass 18400 g) from bovine milk, as produced by NIZO food research (Ede, The Netherlands), was dissolved directly in a buffer solution at pH

2.5 in 5 ml vials for varying protein concentrations ranging from 10 mg ml^{-1} (0.54 mM) up to 200 mg ml^{-1} (11 mM). A citrate-phosphate buffer (i.e. a McIlvaine buffer) was used because of its unmatched pH stability at higher protein concentrations, while a pH of 2.5 was chosen to account for the increase in solution alkalinity due to the buffering effect of the protein upon full dilution and because it also allows for the exact final pH 3 value to be achieved with minimal titration (through the addition of HCl/NaOH). For titration a relatively high concentration of HCl/NaOH (10% w/v) was used in order to minimise the alteration of the desired protein concentration of the solution [10]. Sodium azide was added as an anti-bacterial agent. Sample vials were gently rotated for four hours at room temperature to allow the protein to fully dissolve before being stored at refrigerated temperatures (5°C) for 24 h. Resulting protein concentrations for each sample were determined by UV spectrometry (Cary50 UV-Vis spectrophotometer) at 278 nm with an extinction coefficient of $0.96\text{ cm}^2\text{ mg}^{-1}$ [6]. The pH of each sample was manually titrated to pH 3 by the gradual addition of HCl and/or NaOH (10% w/v), whilst magnetically stirring each sample. All samples were concentration corrected for the addition of HCl and/or NaOH and then rotated for a further four hours and the pH was checked again to ensure a homogenous distribution of the protein and a true pH reading as the protein itself has a buffering effect.

The average secondary structure of the proteins in solution was determined by attenuated total reflectance Fourier transform infrared (ATR FTIR) spectroscopy. It is a suitable and well-documented technique for testing the secondary structure of proteins in solution, including BLG [11]. In this work, we focus on the amide I region of the spectrum, 1700 to 1500 cm^{-1} , which reflects several modes of the peptide backbone: the C=O stretching vibration, bending modes of the N–H group and the C–N stretch [12]. Changes in the absorption in the band give information on the proteins' secondary structure.

Measurements were performed by pipetting samples onto a Bruker Optics Equinox 55 ATR-FTIR, with a diamond module temperature-controlled at 25°C . Scans (256 in total) were made with a 4 cm^{-1} resolution. Due to the detection limits of the instrumentation the lowest protein concentration at which accurate ATR FTIR measurements are possible was 10 mg ml^{-1} . Changes in the spectra due to dimerization are subtle and hard to see in the untreated spectra, see figure 1. Therefore, the 2nd derivative of the spectra was taken in order to enhance the less obvious differences between the spectra measured at different concentrations. OPUS 5 spectroscopy software (Bruker) was used. The 2nd derivative of the spectra was buffer corrected by subtracting the buffer signal and background noise spectrum and then normalised on the total absolute intensity of the 2nd derivative spectrum. An overlay of the normalised 2nd derivative spectra in the amide I region is what is shown in figure 2.

3. Theory

Consider the following reversible dimerisation reaction for BLG,

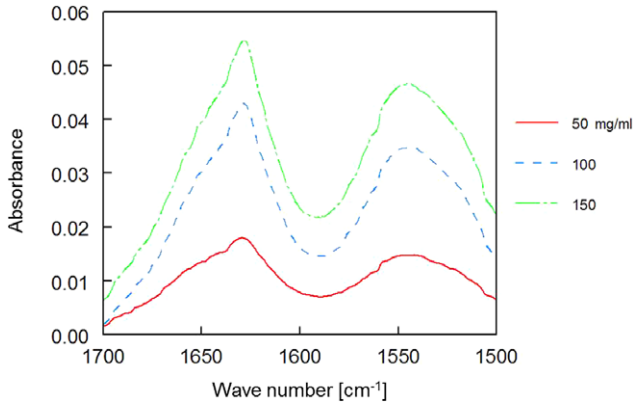


Figure 1. Examples of non-normalised spectra at BLG concentrations of 50, 100 and 150 mg ml⁻¹.

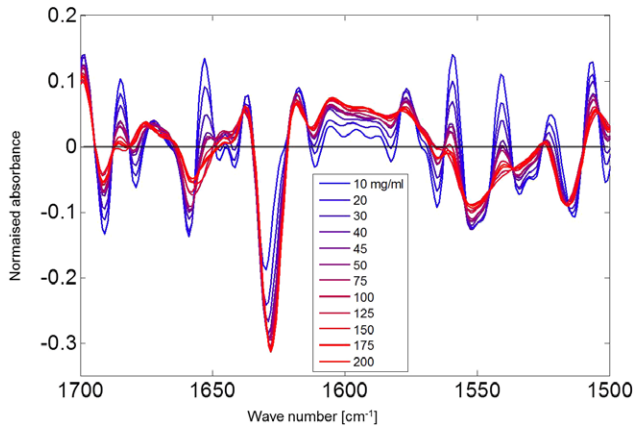


Figure 2. Overlay of the 2nd derivative of the ATR FTIR spectra (normalised on the total absolute intensity in the range 1500–1700 cm⁻¹) in the amide I region (1700–1600 cm⁻¹) for a range of protein concentrations buffered at pH 3 in a McIlvaine buffer (0.2 M Na₂HPO₄ and 0.1 M citric acid).



in which $[M]$ is the molar concentration of monomeric BLG and $[D]$ that of dimeric BLG. The dimension-bearing equilibrium constant K is commonly defined as

$$K = \frac{[D]}{[M]^2} = \frac{1}{2c} \frac{\eta}{(1-\eta)^2} \quad (2)$$

in which the total concentration of protein is $c = [M] + 2[D]$. Here,

$$\eta = \frac{2[D]}{2[D] + [M]} \quad (3)$$

is the fraction of protein molecules in the dimeric state, i.e. the degree of dimerisation. As can be concluded from a glance at the experimental spectra of figure 2, and as can be deduced from equation (2) that in essence represents the law of mass action, the degree of dimerisation η is concentration dependent. The value of K can be determined if one knows η as a function of the overall concentration of proteins in the solution. This is what we will extract from our FTIR spectra, measured for a whole range of concentrations. It is important to

realise, however, that K in equation (2) is a constant only in dilute solution, not at the high concentrations at which we do our experiments. If we insist on using equation (2), then interactions between the proteins make the equilibrium constant K a function of the concentration of protein, c . Indeed, if we ignore this we turn out to underestimate the degree of dimerisation at high concentrations where crowding effects start to play a role [7–9].

Hence, in order to understand and interpret the concentration dependence of the equilibrium constant K , we must deal with the influence of crowding and derive a relation between this parameter, the protein concentration, the degree of dimerization and some measure for the level of crowding that turns out to be the effective volume fraction of the proteins in the solution [7–9]. Here, we outline our model. The first step is to define a model free energy that accounts for (i) an ideal mixing and translational entropy of the monomers and the dimers, (ii) the binding free energy associated with each dimer, and (iii) excluded-volume effects. Volume exclusion we for simplicity deal with at the level of a second virial approximation.

It is convenient to set up the theory in a grand canonical ensemble and write down for our model the grand canonical potential per unit volume and per unit of thermal energy $k_B T$,

$$\begin{aligned} \psi = & \rho_M \log \rho_M v_M - \rho_M - \mu \rho_M + \rho_D \log \rho_D v_D - \rho_D - 2\mu \rho_D \\ & + \varepsilon \rho_D + B_{MM} \rho_M^2 + B_{MD} \rho_M \rho_D + B_{DD} \rho_D^2, \end{aligned} \quad (4)$$

in which ρ_M is the number density of BLG in the monomeric form, ρ_D the number density of dimers, v_M and v_D are interaction volumes that for notational simplicity and without loss of generality we replace by the volume of a single solvent molecule. Furthermore we have $\varepsilon < 0$ for the dimer binding free energy, μ for the chemical potential of the proteins and B_{MM} , B_{MD} , B_{DD} for the second virial coefficients for monomer–monomer, monomer–dimer and dimer–dimer interactions respectively. The second virial coefficients are known quantities if the monomer is modeled as a hard-sphere particle with an effective diameter of σ and the dimer as a hard spherocylinder [14] with an effective diameter σ and length $L = 2\sigma/3$. We choose the length of the spherocylinder such that its effective volume equals that of two monomers. In that case, $B_{MM} = 2\pi\sigma^3/3$, $B_{MD} = \pi\sigma^3$ and $B_{DD} = 13\pi\sigma^3/9$.

Thermodynamic equilibrium implies the grand potential to be minimal. Hence, we minimize the grand canonical potential with respect to ρ_M and ρ_D . This gives two expressions, allowing us to eliminate from one of them the chemical potential μ . This then produces the modified law of mass action in the variables ρ_M and ρ_D . One of the density variables we remove by insisting that the number density of BLG proteins, $\rho_M + 2\rho_D$, is conserved and equal to c . The final result of our calculation, which is the concentration dependent equilibrium constant, is

$$K = K_0 \exp \left[\gamma^3 \left(4\varphi - \frac{2}{3} \varphi \eta \right) \right], \quad (5)$$

where $K_0 = [H_2O]^{-1} e^{-\varepsilon}$ is the equilibrium constant at infinite dilution, $[H_2O]$ the molar concentration of water and φ

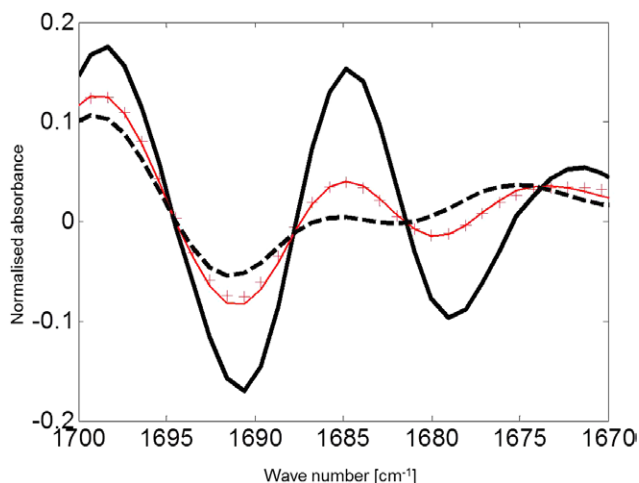


Figure 3. Example of the quality of the applied fit procedure for the spectral data at 40 mg ml^{-1} (symbols). The dashed curve is the data at 200 mg ml^{-1} , assumed to be the dimer spectrum. The bold full curve is the monomer spectrum and is a result of the fitting procedure. The curve approaching the symbols is the best fitting linear combination (see equation (6)) of the monomer and dimer spectra.

$= cM_{\beta}/\rho_{\beta}$ is the volume fraction of protein in the solution, with M_{β} the molar mass of BLG and $\rho_{\beta} = 1440 \text{ mg ml}^{-1}$ the mass density of BLG [13]. Finally, $\gamma = \sigma/\sigma_0$ is the ratio of the effective hard-sphere diameter, σ , which includes the effects of repulsive electrostatic interactions and hydration layers, and the bare, hard-sphere diameter σ_0 . By fitting this equation to the concentration dependent degree of dimerisation as we shall shortly show can be determined from the ATR-FTIR measurements, we are able to determine the values of γ and ϵ (or, equivalently, K_0). Note that any influence of higher order virials and of the not exactly spherical shape of the monomer units are absorbed into the value of γ .

Equation (5) tells us that interactions between the proteins increase the equilibrium constant. The reason is that by dimerising the proteins increase the free volume of the solution. This becomes more important the larger the amount of volume the proteins take up, i.e. a direct result of (self) crowding. As we shall show in the following section, simply putting $K = K_0$ and ignoring the influence of crowding on the dimerization equilibrium cannot explain our data.

4. Results

4.1. Raw data

For the purpose of illustration, in figure 1 some zeroth-derivative, uncorrected spectra are shown in the range of wave numbers studied. Two absorbance peaks are observed, one at 1625 cm^{-1} and one at 1540 cm^{-1} . The former, the so-called amide I peak, is due to the C=O stretching vibration of the C=O bond in the peptide backbone of the protein. The amide II peak at 1540 cm^{-1} is due to the C–N vibration and the N–H bending modes. Both are sensitive to the hydrogen-bonded structure in the direct surroundings, involving the carbonylic O atom in the case of the amide I peak, and the secondary

amine (NH) group in the case of the amide II peak [12, 15]. Figure 1 not only shows that the absorbance increases non-linearly with increasing protein concentration but also that there are subtle changes in the spectra themselves.

4.2. Second derivative data

In order to make subtle changes in the obtained spectra visible, we calculated the second derivative spectra from our data. The normalised second derivative spectra are given in figure 2. Clearly, with increasing concentration the detailed shape of the spectra changes. Still, there are a number of crossing points where the intensity of the spectra at different concentrations remains invariant. These are so-called isosbestic points. The existence of isosbestic points, combined with a changing shape of the spectra with increasing concentration, suggests two coexistent conformations of the proteins that gain or lose prevalence relative to each other with varying concentration and is in agreement with the reversible dimerisation of BLG that we presumed to occur. At the wave numbers of the isosbestic points, the second derivative of the specific extinction coefficient with respect to the wave number of the two types of protein conformations is the same.

However, the spectra cannot be interpreted entirely in terms of a population of two conformers, because in some ranges of wave numbers, e.g. from 1630 to 1660 cm^{-1} , the wave numbers of the crossing point shift with concentration. This means that the folding of monomers and dimers is not nor completely conserved when dimerization takes place. Because in only a small part of the wave number range spectra evolve around shifting crossing points, we process the spectra assuming that each of them is the weighted sum of two spectra, one representing a ‘dimer spectrum’ and one a ‘monomer spectrum’. The spectrum of the highest concentration is taken as the dimer spectrum, because in concentration range 100 – 200 mg ml^{-1} the normalized spectra are practically identical and therefore full dimerisation has arguably taken place. The monomer spectrum is not directly available from our set of measurements, because even at the lowest concentration where data was available, 10 mg ml^{-1} , the spectra are still concentration dependent. However, we shortly show that the monomer spectrum can be obtained by a different method.

In order to determine the value of K at concentration c , we express the spectrum at this concentration, $S(c)$, as a linear combination of the dimer spectrum S_D and a ‘monomer spectrum’ S_M , so

$$S(c) = [1 - \eta(c)] S_M + \eta(c) S_D \quad (6)$$

in which the fraction proteins in dimeric form $\eta(c)$ is concentration dependent and by given by equation (3). There are two unknowns, that is, $\eta(c)$ and S_M . We take S_D to be the spectrum at the highest concentration measured. In order to extract S_M from the data, we carry out a fitting procedure involving the measured spectra at all concentrations. The fitting procedure consists of searching the unknown spectrum, which is in linear combination with S_D best able to reproduce all these spectra. The limitation we impose on the unknown S_M is that its correlation with S_D is minimal, or, in mathematical terms, we seek

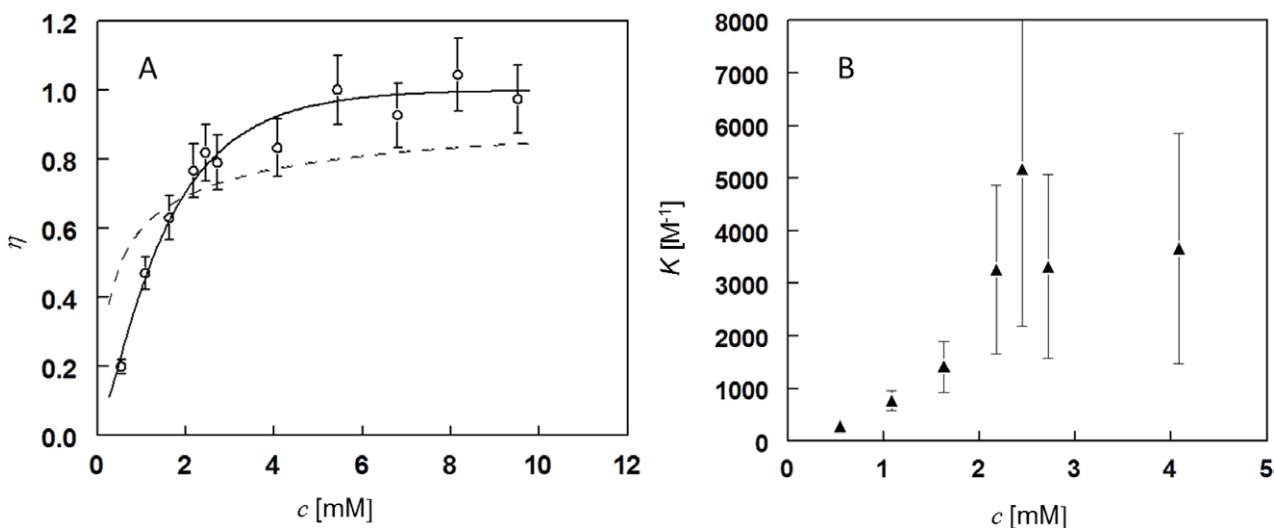


Figure 4. (A) The degree of dimerisation η (obtained by fitting equation (6) to the spectra in figure 2) versus the molar concentration c . The full curve is the best fit of equation (5) to the data. Best fitting parameters are $K_0 = 1.8 \cdot 10^2 \text{ M}^{-1}$ and $\gamma = 3.10$. Dashed curve: best fit for ideal mass action, i.e. without allowing for molecular crowding ($\gamma \equiv 0$, and the best fitting value of $K_0 = 18.4 \cdot 10^2 \text{ M}^{-1}$). (B) The equilibrium constant K , calculated from the experimental data using equation (2), as a function of the protein molar concentration.

the vector that is orthogonal to S_D . This limitation can also be formulated as the demand that the shapes of the dimer and monomer spectra should be as ‘different’ as possible while still reproducing the data. The weight $\eta(c)$ and the entire spectrum S_M between 1500 and 1700 cm^{-1} are adjustable parameters in the fitting procedure. Figure 3 shows an example of the fit results. It should be noted that the ‘monomer spectrum’ obtained in this way is the spectrum that is orthogonal to the dimer spectrum and therefore dependent on the assumption of a monomer–dimer equilibrium. This means that it is not unique. Strictly speaking, if this procedure were carried out in an imaginary experimental situation in which monomers were in equilibrium with e.g. dimers and trimers, a different ‘monomer spectrum’ could be the result.

The results for $\eta(c)$ and S_M are in the figures 4 and 5, respectively. The best fitting values were $3.1 (\pm 0.5)$ for γ and $1.84 (\pm 0.5) \cdot 10^2 \text{ M}^{-1}$ for K_0 . The strong dependence of $\eta(c)$ on the concentration at low concentrations reflects the strong tendency to form dimers with increasing concentration. At about 20 mg ml^{-1} (1.6 mM) half the molecules are in the dimeric state. When not allowing for molecular crowding no satisfactory fit can be obtained (dashed line in figure 4). This indicates that ideal mass action cannot solely explain the enhancement of dimerization with increasing concentration. Another way to illustrate the effect of crowding is to consider the concentration dependence of the equilibrium constant K , shown in figure 4(B). K increases strongly with increasing molar protein concentration, reflecting an increasing tendency to form dimers at higher concentration. The error in K becomes unacceptably high when η approaches unity, as a result of the factor $(1 - \eta)$ [2] in the denominator of equation (2). Therefore, this method is not suitable to generate quantitative data at concentrations where η is close to unity.

The second derivative spectra in figure 5 show significant difference at the positions of both the amide I and amide II peaks, reflecting changes in the hydrogen bonding of the N–H

and the C=O groups of the peptide bond, and implying that the proteins in the monomeric state and in the dimeric state have different conformations.

5. Discussion

The two main results from the concentration-dependent IR spectra that we obtained on our solutions of BLG are a value for the equilibrium constant of the dimerization at infinite dilution K_0 , and a spectrum of a BLG solution at infinite dilution. We consider the result for, and the method by which we obtained the equilibrium constant the main aim of this work, and so will discuss this in some detail. The value we find for K_0 , $1.84(\pm 0.5) \cdot 10^2 \text{ M}^{-1}$, is considerably smaller than reported previously [5, 16]. Unfortunately, a direct comparison with earlier values is complicated by the extreme sensitivity of the dimerisation constant to the ionic strength and the specific type of salt that is added [16]. Indeed, under identical experimental conditions, the dimerisation constant is found to increase by over a factor of 10^3 if instead of 20 mM NaCl , 20 mM NaClO_4 is added as salt, while a 10-fold increase in the concentration of NaCl leads to an increase in the dimerisation constant by a factor of 100. Moreover, results obtained by different experimental methods differ by almost a factor 3 [5]. Complicating matters even further, as our results (figure 4) suggest, is that the bare dimerisation constant can only be accurately determined by equation (2) at very low concentrations $\ll 10 \text{ mg ml}^{-1}$ because of the effect of crowding. For concentrations above 50 mg ml^{-1} there is the other issue of the experimental error in the value of η , which becomes very influential when it approaches the value of unity.

Whilst a direct comparison with other experiments is difficult unless the experimental conditions are identical, we can attempt a comparison with the result of an experiment that was performed under somewhat *similar* experimental conditions.

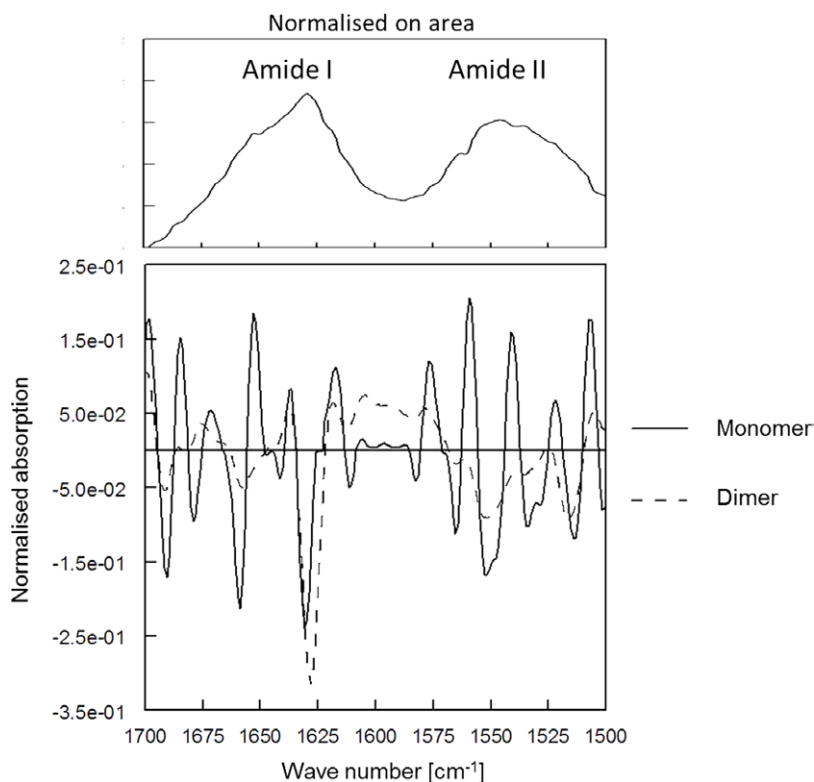


Figure 5. Result of fitting equation (6) to the data of figure 2 for the monomer spectrum S_M , indicated by the full line. The dimer spectrum S_D indicated by the dashed line was held constant and equal to the spectrum at the highest concentration of 200 mg ml^{-1} . In order to identify which spectral features undergo changes on dimerization, a representative raw spectrum (50 mg ml^{-1}) is shown as well.

Sakurai *et al* [16] found a dimerization constant of $K_0 = 1.79 (\pm 0.36) \cdot 10^5 \text{ M}^{-1}$ by performing sedimentation equilibrium experiments over a concentration range of $0.1\text{--}2 \text{ mg ml}^{-1}$ at pH 3 and 1 M of NaCl. Their dimerisation constant is a factor 100–350 larger than ours, which we determined at a BLG concentration between 10 and 50 mg ml^{-1} , at a fixed pH of 3 and $0.2 \text{ M Na}_2\text{HPO}_4$ and 0.1 M citric acid, corresponding to high ionic strength. While it seems difficult to reconcile this large discrepancy, it is in fact of the same order of the difference in the dimerisation constant that Sakurai *et al* observe upon switching from NaCl to NaClO_4 .

There are a number of reasons why we believe the difference in dimerisation constant between two experiments are real and directly linked with the precise experimental conditions. First, BLG dimer formation relies on a subtle balance of hydrophobic interactions at the interface of the two BLG monomers in the dimer, the formation of 12 inter-protein hydrogen bonds and the electrostatic screening of the charges present on the dimer interface [16]. This subtle balance may well be shifted by the presence of non-inert trivalent citrate anions, and possibly also by multivalent phosphate anions if present in the solution. Second, the dimerisation constant is a very sensitive parameter, as it varies exponentially with the dimer binding free energy. As a consequence, differences of a factor of 100 in the binding constant K_0 correspond to modest variations of about $4 k_B T$ in the binding free energy.

We recall that in our model the binding free energy in units of thermal energy is directly related to K_0 via the relation $\varepsilon = \ln(K_0 [\text{H}_2\text{O}])$, where $[\text{H}_2\text{O}] = 55.5 \text{ M}$ is the molar

concentration of water. Hence, we find a dimer binding free energy of $\varepsilon = 9.2 (\pm 0.1)$ in units of $k_B T$. This $9 k_B T$ has to be compared to the value of about $14 k_B T$ that would be consistent with the data of Sakurai *et al* [16]. The small difference can plausibly be explained by ionic bonding effect due to the presence of multivalent ions, although obviously this needs to be confirmed by a detailed calculation, which is outside of the scope of this work.

Finally, for the ratio of the effective and hard-core radius of the proteins γ we find an average value of $\gamma = 3.1 \pm 0.5$, which suggests that the effective radius, which includes the effect of electrostatic interactions between the proteins, equals approximately 3 times the bare hard-sphere radius of 1.7 nm . This suggests that electrostatic and other interactions, which may include a hydration layer bound to the protein surface, extend approximately 3 nm beyond the hard-sphere surface. This seems acceptable not least since γ accounts also for higher order virial coefficients neglected in the theory. The precise value of γ is very sensitive to the choice of the bare radius of BLG monomer, because the radius determines the conversion of concentration in mass per volume (c) to volume fraction (ϕ). A more detailed interpretation of this value for γ is therefore not feasible on the basis of the available data.

6. Conclusions

We have shown that a concentration-dependent change in average protein conformation due to an increasing degree

of dimerisation of beta-lactoglobulin (BLG) can be probed experimentally using ATR FTIR measurements at different BLG concentrations. Furthermore, we showed that a dimerisation model that accounts for the influence of self-crowding, which becomes important at high protein concentrations, can be fitted to the relation that we find between the degree of dimerization and the concentration of the protein. This resulted in a dimerisation constant of $1.84 (\pm 0.5) \cdot 10^2 \text{ M}^{-1}$ and a corresponding dimer binding free energy of ϵ of $9.2 k_B T$. The value of the dimerization constant that we find is considerably lower than those reported earlier in the literature. We tentatively ascribe this discrepancy to a high sensitivity of the molecular dimerization process to types of buffer salts used. The effective hard-core radius of the proteins that we find in order to explain the concentration dependence of the dimerisation constant is 3.1 times the bare molecular radius of BLG of 1.7 nm. This we ascribe to the impact of electrostatic interactions between the proteins and the presence of a hydration shell bound to the proteins.

References

- [1] Bryant C M and McClements D 1998 *Trends Food Sci. Technol.* **9** 143
- [2] Zhu D, Damodaran S and Lucey J A 2008 *J. Agric. Food Chem.* **56** 7113
- [3] Verheul M, Pedersen J S, Roefs S P F M and de Kruif K G 1999 *Biopolymers* **49** 11
- [4] Gottschalk M, Nilsson H, Roos H and Halle B 2003 *Protein Sci.* **12** 2404
- [5] Mercadante D, Melton L D, Norris G E, Loo T S, Williams M A, Dobson R C and Jameson G B 2012 *Biophys. J.* **103** 303
- [6] Bhattacharjee C and Das K P 2000 *Eur. J. Biochem.* **267** 3957
- [7] Zimmerman S B and Minton A P 1993 *Annu. Rev. Biophys. Biomol. Struct.* **22** 27
- [8] Ellis R J 2001 *Trends Biochem. Sci.* **26** 597
- [9] Phillip Y and Schreiber G 2013 *FEBS Lett.* **587** 1046
- [10] Croguennec T, Molle D, Mehra R and Bouhallab S 2004 *Protein Sci.* **13** 1340
- [11] Koenig J and Tabb D 1980 *Analytical Applications of FT-IR to Molecular and Biological Systems, NATO Advanced Study Institutes Series* vol 57 ed J Durig (Netherlands: Springer) pp 241–255
- [12] Barth A 2007 *Biochim Biophys. Acta* **1767** 1073
- [13] Fischer H, Polikarpov I and Craievich A F 2004 *Protein Sci.* **13** 2825
- [14] Onsager L 1949 *Ann. NY Acad. Sci.* **51** 627
- [15] Barth A and Zscherp C 2002 *Q. Rev. Biophys.* **35** 369
- [16] Sakurai K, Oobatake M and Goto Y 2001 *Protein Sci.* **10** 2325